Cell

MTERF3 Is a Negative Regulator of Mammalian mtDNA Transcription

Chan Bae Park,[1] Jorge Asin-Cayuela,[1] Yolanda Cámara,[1] Yonghong Shi,[1] Mina Pellegrini,[1] Martina Gaspari,[1] Rolf Wibom,[1] Kjell Hultenby,[1] Hediye Erdjument-Bromage,[2] Paul Tempst,[2] Maria Falkenberg,[1] Claes M. Gustafsson,[1,*] and Nils-Göran Larsson[1,*]
[1] Department of Laboratory Medicine, Karolinska Institutet, S-141 86 Stockholm, Sweden
[2] Molecular Biology Program, Memorial Sloan-Kettering Cancer Center, New York, NY 10021, USA
*Correspondence: claes.gustafsson@ki.se (C.M.G.), nils-goran.larsson@ki.se (N.-G.L.)
DOI 10.1016/j.cell.2007.05.046

SUMMARY

Regulation of mammalian mtDNA gene expression is critical for altering oxidative phosphorylation capacity in response to physiological demands and disease processes. The basal machinery for initiation of mtDNA transcription has been molecularly defined, but the mechanisms regulating its activity are poorly understood. In this study, we show that MTERF3 is a negative regulator of mtDNA transcription initiation. The MTERF3 gene is essential because homozygous knockout mouse embryos die in midgestation. Tissue-specific inactivation of MTERF3 in the heart causes aberrant mtDNA transcription and severe respiratory chain deficiency. MTERF3 binds the mtDNA promoter region and depletion of MTERF3 increases transcription initiation on both mtDNA strands. This increased transcription initiation leads to decreased expression of critical promoter-distal tRNA genes, which is possibly explained by transcriptional collision on the circular mtDNA molecule. To our knowledge, MTERF3 is the first example of a mitochondrial protein that acts as a specific repressor of mammalian mtDNA transcription initiation in vivo.

INTRODUCTION

Deficient oxidative phosphorylation plays an important role in various types of human pathologies, such as inherited mitochondrial diseases (Smeitink et al., 2001), age-associated common diseases (Lin and Beal, 2006), and aging (Lin and Beal, 2006; Trifunovic, 2006). Mitochondrial function must be regulated in response to a variety of metabolic demands occurring in normal physiological processes. The large number of proteins necessary for oxidative phosphorylation and the dual genetic origin of these proteins make regulation complex. An increase in oxidative phosphorylation capacity necessitates a concerted activation of transcription of both mtDNA and nuclear genes.

The basal mitochondrial transcription machinery has been molecularly defined, and all of the necessary components are encoded by nuclear genes and imported into mitochondria. A combination of three proteins, i.e., mitochondrial RNA polymerase (POLRMT), mitochondrial transcription factor A (TFAM), and mitochondrial transcription factor B1 or B2 (TFB1M or TFB2M) are sufficient and necessary for specific initiation of transcription from mtDNA promoters in vitro (Falkenberg et al., 2002). TFAM is an abundant high-mobility-group-box protein that has at least two separate functions in mammalian mitochondria. It has the capacity to bind and bend DNA (Parisi and Clayton, 1991) and likely contributes to the packaging of mtDNA into nucleoids (Ekstrand et al., 2004). A direct role for TFAM in mtDNA maintenance is further supported by the observation that knockout of TFAM leads to loss of mtDNA (Larsson et al., 1998) and overexpression of TFAM upregulates mtDNA copy number in the mouse (Ekstrand et al., 2004). In addition to its role as a structural protein, TFAM also functions as a basal transcription factor (Dairaghi et al., 1995), and not even abortive transcription can occur in its absence (Gaspari et al., 2004). Both TFB1M and TFB2M form stable heterodimers with POLRMT, but TFB2M is at least an order of magnitude more active than TFB1M in promoting in vitro transcription initiation (Falkenberg et al., 2002). Interestingly, TFB1M and TFB2M are homologous to bacterial dimethyladenosine transferases and may therefore also have a role in rRNA modification (Falkenberg et al., 2002; Seidel-Rogol et al., 2003). The distinct in vivo roles for TFB1M and TFB2M remain to be elucidated.

The nuclear respiratory factors (NRF1 and NRF2) control the basal expression of many nuclear genes encoding mitochondrial proteins (Scarpulla, 2006; Wu et al., 1999). There is accumulating evidence that the PGC-1 group of nuclear transcription factors (Pgc1α, Pgc1β, and PRC) are master regulators that can be induced by environmental stimuli to activate the expression of nuclear genes encoding proteins necessary for oxidative phosphorylation (Lin et al., 2005; Scarpulla, 2006). Pgc1α is the most

studied member of this group of transcription factors and disruption of its gene leads to decreased expression of TFAM (Lin et al., 2004). Increased expression of Pgc1α can directly activate expression of TFAM and thereby provides a pathway to increase copy number and overall expression of mtDNA (Wu et al., 1999). However, TFAM is a very abundant protein fully coating mtDNA, and may therefore not be ideal for rapid adjustment of mtDNA transcription according to metabolic needs. It therefore appears likely that additional factors must regulate the basal mtDNA transcription machinery to allow fine-tuning in response to demands for oxidative phosphorylation capacity.

In this paper, we show that a previously uncharacterized mammalian protein denoted mitochondrial transcription termination factor 3 (MTERF3) (Linder et al., 2005) is located in mitochondria where it interacts with the mtDNA promoter region and functions as a transcriptional repressor. Loss of MTERF3 is embryonically lethal, and tissue-specific knockout of *Mterf3* in the heart leads to increased transcription initiation on both strands of mtDNA, decreased steady-state levels of promoter-distal transcripts, and, eventually, mitochondrial dysfunction. In conclusion, MTERF3 is, to our knowledge, the first example of a mitochondrial protein that acts as a specific negative regulator of mammalian mtDNA transcription initiation in vivo.

RESULTS

MTERF3 Is a Mitochondrial Protein

Bioinformatics analyses were used to predict subcellular localization of the human MTERF3 protein. The three software programs used—MitoProt (99.6%), TargetP (92.1%), and PSORT (73.9%)—gave a high probability for mitochondrial localization. We performed northern blot analyses and found that *Mterf3* is ubiquitously expressed, consistent with the prediction that the *Mterf3* gene encodes a mitochondrial protein (Figure 1A). We transfected HeLa cells with plasmids encoding a fusion protein consisting of MTERF3 fused at its carboxy terminus to green fluorescent protein (MTERF3-GFP). The intracellular localization of MTERF3-GFP overlapped perfectly with mitochondria labeled with the fluorophore mitotracker (Figure 1B). Next, we studied import of recombinant [^{35}S]-methionine-labeled human MTERF3 into isolated rat liver mitochondria (Figure 1C). Import of full-length MTERF3 into mitochondria generated a protein species of lower molecular weight, showing that the targeting sequence is cleaved after import. The generation of this processed MTERF3 protein was inhibited by the addition of the uncoupler CCCP, consistent with the fact that mitochondrial protein import is typically dependent on a potential across the inner mitochondrial membrane. Additionally, the processed MTERF3 protein was resistant to trypsin treatment, whereas the full-length MTERF3 protein was degraded. These findings show that MTERF3 is a mitochondrial protein.

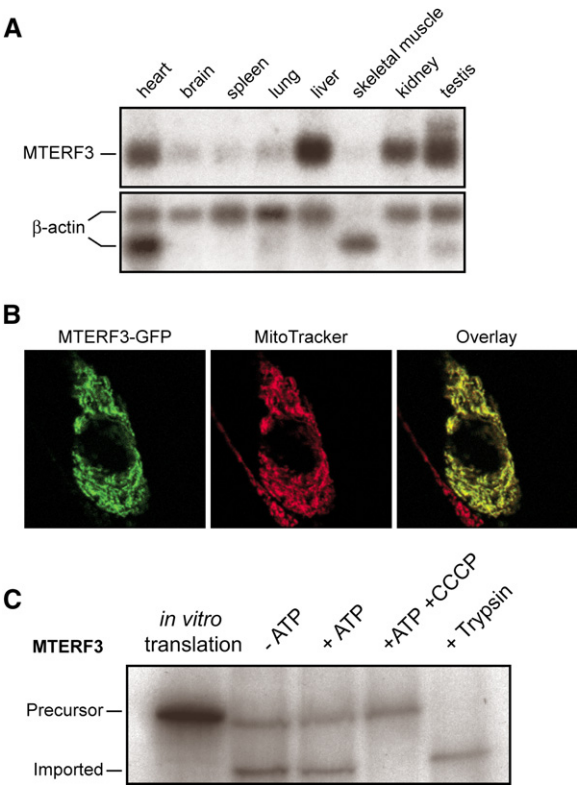

Figure 1. Expression of *Mterf3* and Mitochondrial Localization of the MTERF3 Protein

(A) Northern blot analysis of *Mterf3* expression in different mouse tissues. A single *Mterf3* transcript of ~1.8 kb was present in all investigated tissues. The *Mterf3* transcript was also detectable in skeletal muscle after prolonged exposure of the blots. β-*actin* was used for loading control.

(B) Confocal microscopy to determine subcellular localization of human MTERF3 in HeLa cells transfected with plasmids encoding GFP-tagged human MTERF3 (MTERF3-GFP). MitoTracker specifically stains mitochondria.

(C) Import of radiolabeled MTERF3 protein into isolated rat mitochondria.

MTERF3 Is Essential for Mouse Embryonic Development

We generated a conditional knockout allele for *Mterf3* by homologous recombination in embryonic stem (ES) cells (Figures 2A and 2B). The allele was transmitted through the mouse germ line and the resulting heterozygous (*Mterf3*$^{+/neo\text{-}loxP}$) mice were mated with *Flp*-deleter mice (Rodriguez et al., 2000) to remove the neomycin resistance gene by *Flp-Frt*-mediated recombination in vivo, thus generating heterozygous mice with a *loxP*-flanked *Mterf3* allele (*Mterf3*$^{+/loxP}$). The *Mterf3*$^{+/loxP}$ mice were crossed to β-*actin-cre* mice (Larsson et al., 1998) and heterozygous knockouts (*Mterf3*$^{+/-}$) were obtained (Figure 2C). Next, we intercrossed *Mterf3*$^{+/-}$ mice, but no homozygous knockouts (*Mterf3*$^{-/-}$) were born. Analysis of staged embryos revealed that the *Mterf3*$^{-/-}$ embryos

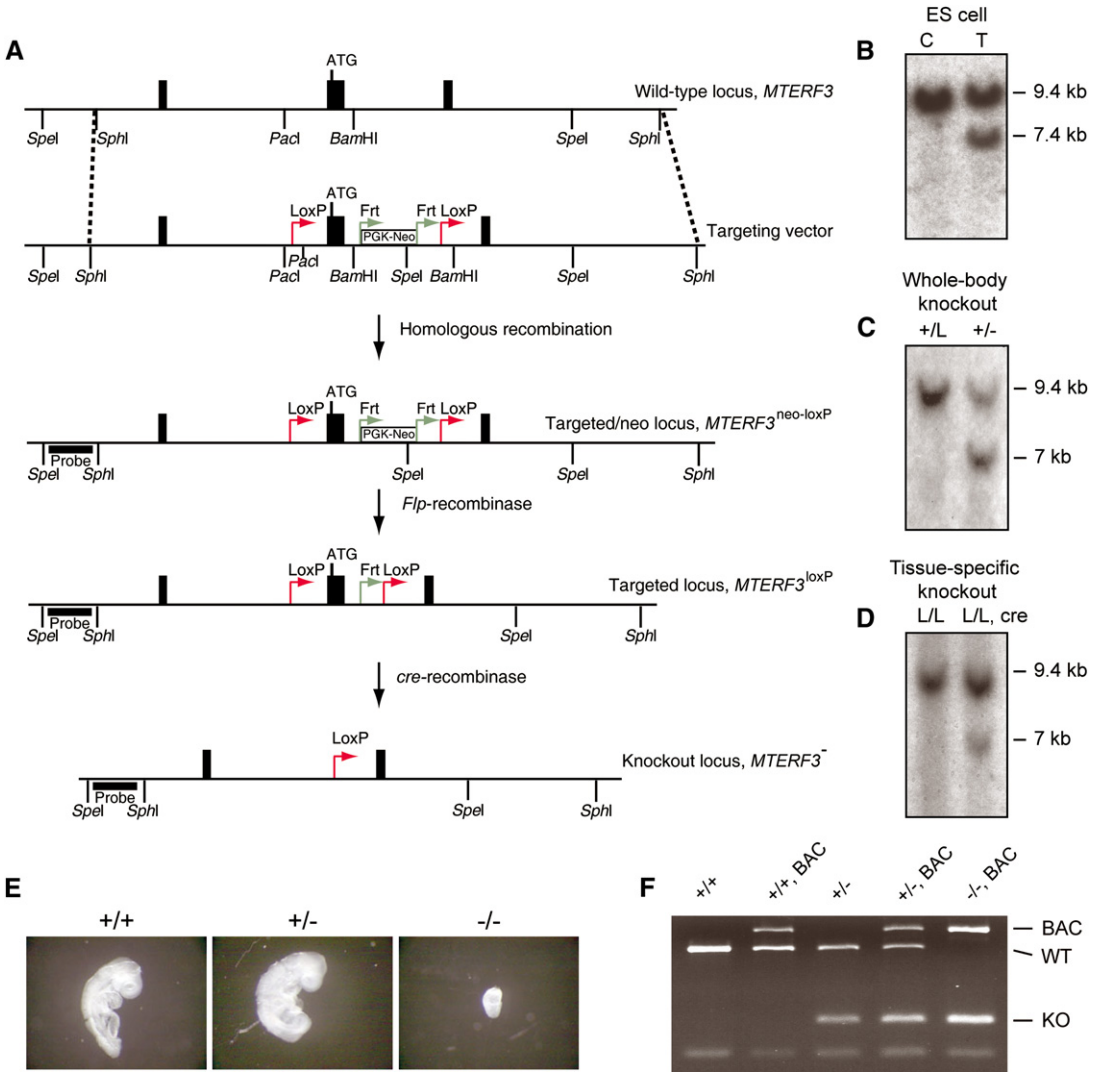

Figure 2. Disruption of *Mterf3* and Rescue of Knockout Phenotype

(A) Restriction map of the 5′ region of the wild-type *Mterf3* locus (*Mterf3*), the targeting vector, the *Mterf3* locus after homologous recombination (*Mterf3*$^{neo\text{-}loxP}$), the *Mterf3* locus after *Flp*-recombinase-mediated excision of *PGK-neo* gene (*Mterf3*^{loxP}), and knockout *Mterf3* locus (*Mterf3*$^{-}$). The thick line indicates the probe used to screen for homologous recombination and knockout allele.

(B) Analysis of control (C) and targeted (T) ES cells. Digestion of ES cell DNA with SpeI generates a novel fragment of 7.4 kb in *Mterf3*$^{+/neo\text{-}loxP}$ clones.

(C and D) Digestion of heart genomic DNA with SpeI generates a 7 kb knockout fragment in *Mterf3*$^{+/-}$ mice (+/−) and tissue-specific knockout mice (L/L, cre; genotype *Mterf3*$^{loxP/loxP}$; +/*Ckmm-cre*).

(E) Morphology of wild-type (+/+), heterozygous (+/−), and homozygous knockout (−/−) E8.5 embryos.

(F) A fragment of *Mterf3* cDNA was synthesized from kidney RNA by PCR and digested with PstI (Figure S1B). DNA fragments of expected sizes were detected in mice heterozygous for the *BAC-Mterf3*^{M} transgene (BAC) that had a wild-type (+/+), heterozygous knockout (+/−), or homozygous knockout (−/−) *Mterf3* genotype. DNA fragments corresponding to *BAC-Mterf3* (BAC), wild-type *Mterf3* (WT), and knockout *Mterf3* (KO) are indicated.

were much smaller than wild-type embryos at embryonic day 8.5 (E8.5) (Figure 2E). No viable *Mterf3*$^{-/-}$ embryos were recovered at E10.5. These results are consistent with previous reports showing that abolished oxidative phosphorylation typically results in embryonic lethality at ~E8.5 (Hance et al., 2005; Larsson et al., 1998). We confirmed that the embryonic lethality was due to the absence of a functional *Mterf3* gene by performing genetic rescue experiments. A bacterial artificial clone (BAC) containing the *Mterf3* gene was engineered to generate a synonymous codon change abolishing a PstI restriction site in the *Mterf3* coding sequence (see Figure S1 in the Supplemental Data available with this article online). This modified BAC was injected into pronuclei of fertilized oocytes to obtain heterozygous transgenic (+/*BAC-Mterf3*) mice. We performed crosses and obtained viable and apparently normal mice of the genotype *Mterf3*$^{-/-}$; +/*BAC-Mterf3*, showing that the homozygous *Mterf3* knockouts

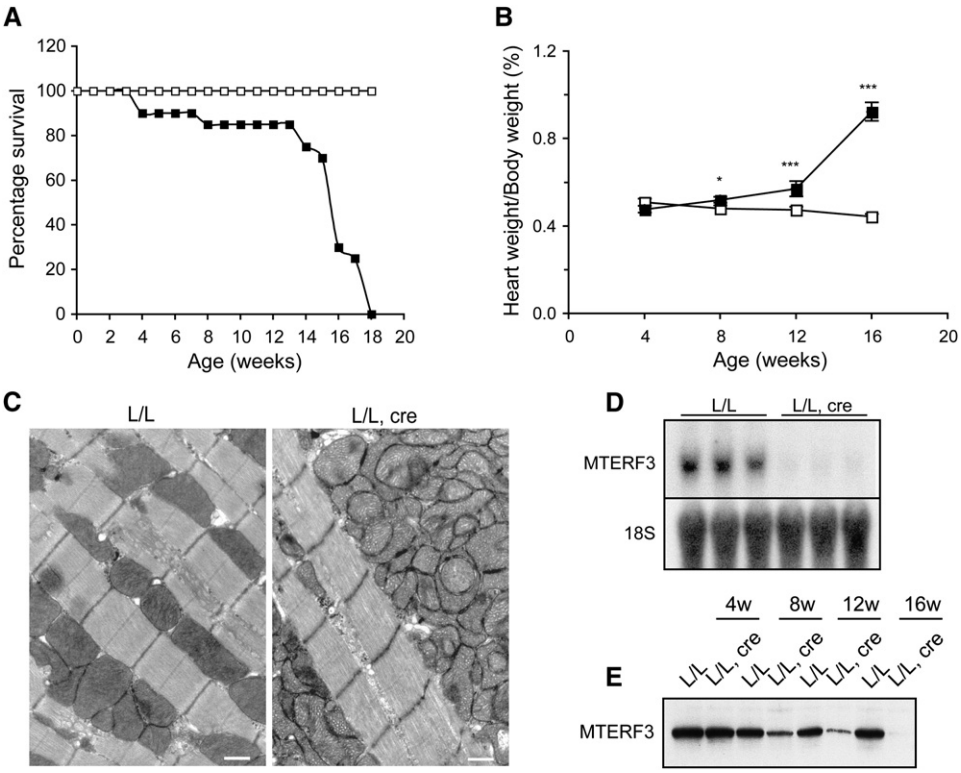

Figure 3. Phenotypic Characterization of Tissue-Specific Knockout Mice

(A) Survival curve for control (L/L, genotype *Mterf3*$^{loxP/loxP}$) mice (n = 60) and tissue-specific knockout (L/L, cre, genotype *Mterf3*$^{loxP/loxP}$; +/*Ckmm-cre*) mice (n = 20). Controls, open squares; knockouts, filled squares.

(B) Heart weight/body weight ratios in control and knockout mice at different ages. *$p < 0.05$; ***$p < 0.001$, Student's t test. All error bars indicate SEM. Controls, open squares; knockouts, filled squares.

(C) Electron micrographs of myocardium from control (n = 3) and tissue-specific knockout (n = 3) mice.

(D) Northern blot analysis of *Mterf3* transcript level in the RNA isolated from the heart of control and tissue-specific knockout mice. *18S* ribosomal RNA (18S) was used as loading control.

(E) Western blot analysis of MTERF3 levels from the heart of control and tissue-specific knockout mice at different ages in weeks (w).

can be rescued by reintroduction of the *Mterf3* gene (Figure 2F).

Loss of MTERF3 Causes Severe Mitochondrial Dysfunction

We bred *Mterf3*^{loxP} mice to transgenic mice expressing *cre*-recombinase from the muscle creatinine kinase promoter (Hansson et al., 2004) to disrupt *Mterf3* in heart (Figure 2D) and skeletal muscle. These tissue-specific knockout animals had a dramatically shortened life span with a maximal longevity of 18 weeks (Figure 3A). We observed a gradual increase of both relative (Figure 3B) and absolute heart size (Figures S2A and S2B) in the tissue-specific knockouts. Electron micrographs of heart tissue from terminal-stage *Mterf3* knockouts revealed abundant abnormal mitochondria, consistent with severe respiratory chain deficiency (Figure 3C). Quantification of mitochondrial volume density showed an increase in relative mitochondrial mass in hearts of *Mterf3* knockouts in comparison with controls at age 12 weeks (143% ± 2%; mean ± SEM) and 16 weeks (192% ± 4%; mean ± SEM).

The *Mterf3* transcript was absent in heart of end-stage tissue-specific knockouts (Figure 3D). Western blots showed a gradual decline of MTERF3 protein levels with time in hearts of the tissue-specific knockouts (Figure 3E). Skeletal muscle had normal morphological appearance at age 16 weeks (not shown). We have previously generated mice with tissue-specific respiratory chain dysfunction selectively in heart (Li et al., 2000), skeletal muscle (Wredenberg et al., 2002), or both of these tissues (Hansson et al., 2004; Wang et al., 1999) by conditional knockout of the gene encoding TFAM. These previous studies have demonstrated a marked difference between tissues in their ability to tolerate mtDNA depletion, with much earlier onset of respiratory chain deficiency in heart than in skeletal muscle. This discrepancy between the two tissues likely explains why we observed no obvious phenotype in skeletal muscle of the *Mterf3* knockouts at the end of their lives. The cause of death in the *Mterf3* tissue-specific knockout mice was thus mitochondrial cardiomyopathy caused by the absence of MTERF3 protein in heart.

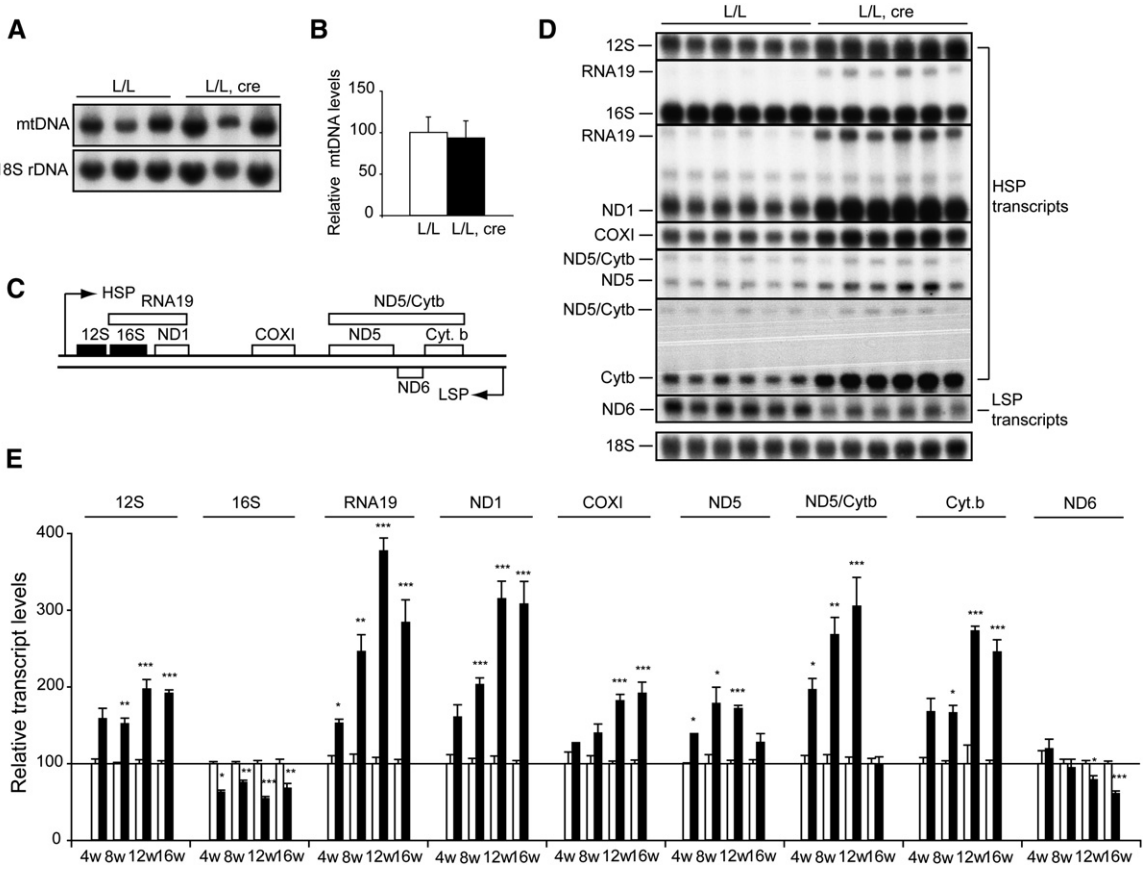

Figure 4. Steady-State Levels of mtDNA and Mitochondrial Transcripts in the Heart of Tissue-Specific Knockout Mice

(A) Southern blot analysis of levels of mtDNA in wild-type and *Mterf3* knockout hearts.

(B) Quantification of mtDNA levels in wild-type (n = 6; white bar) and *Mterf3* knockout (n = 6; black bar) hearts.

(C) Map indicating analyzed rRNA and protein-coding mitochondrial transcripts. The 12S rRNA (12S), 16S rRNA (16S), RNA19, ND1, COXI, ND5, and Cyt b transcripts are transcribed from the heavy-strand promoter (HSP). The ND6 transcript is transcribed from the light-strand promoter (LSP).

(D) Northern blot analyses of mitochondrial transcripts in control (L/L) and *Mterf3* knockout (L/L, cre) hearts at 16 weeks of age (pairs of animals analyzed, n = 6). Nuclear 18S ribosomal RNA (18S) was used for loading control.

(E) Quantification of mitochondrial transcript levels of control (white bars) and tissue-specific knockout (black bars) mice at different ages in weeks (w).

*p < 0.05; **p < 0.01; ***p < 0.001; Student's t test. All error bars indicate SEM.

Loss of MTERF3 Causes Increased Steady-State Levels of mtDNA Transcripts

The levels of mtDNA were normal in end-stage *Mterf3* knockout hearts (Figures 4A and 4B). We investigated the steady-state levels of mRNAs generated by transcription from the light-strand promoter (LSP) and the heavy-strand promoter (HSP) of mtDNA in *Mterf3* knockout hearts at the ages of 4, 8, 12, and 16 weeks (Figures 4C–4E). We found a general increase in levels of HSP transcribed mRNAs in heart, whereas the levels of ND6 transcripts, the only mRNA transcribed from LSP, were decreased in tissue-specific knockouts (Figures 4C–4E). Interestingly, the levels of mRNAs transcribed from HSP were more elevated in old knockouts in comparison with young knockouts (Figure 4E), mirroring the gradual decrease in the MTERF3 protein levels between the ages of 4 and 16 weeks (Figure 3E). The mitochondrial rRNA genes are transcribed from HSP, and we found elevated steady-state levels of the 12S rRNA transcript in hearts from knockouts at all investigated ages (Figure 4E). The levels of 16S rRNA were decreased, but the levels of RNA19, which encompass 16S rRNA and ND1, were increased (Figure 4E). This indicates that impaired processing of RNA 19 explains the observed decrease of 16S rRNA. We also found increased levels of another precursor transcript containing ND5/Cyt b sequences (Figures 4D and 4E).

Next, we assessed steady-state levels of tRNAs in hearts of 16-weeks-old *Mterf3* knockouts (Figure 5). The steady-state levels of tRNAs transcribed from HSP were highly increased, with the exception of the most promoter-distal tRNA gene ($tRNA^T$; Figures 5A–5C). The levels of tRNAs transcribed from LSP were increased if the gene had a promoter-proximal location, and decreased if the

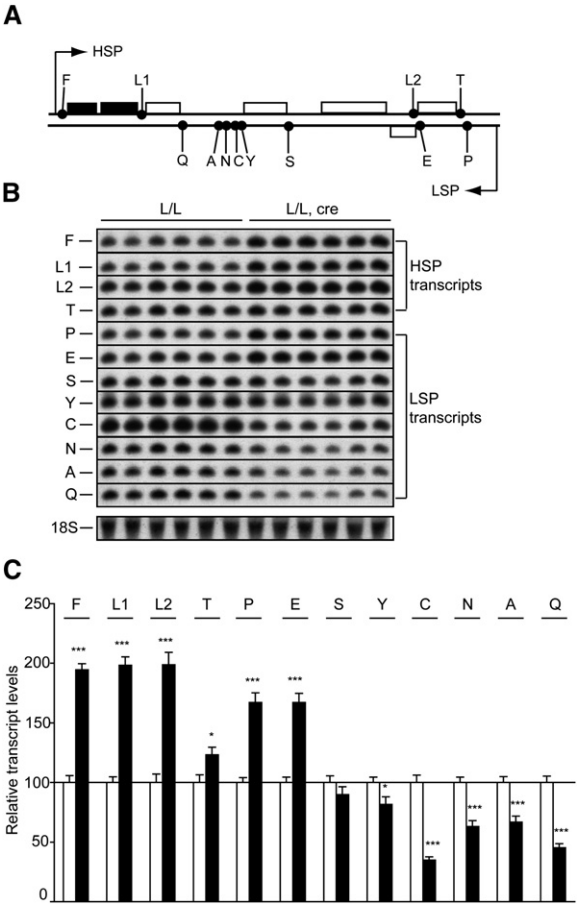

Figure 5. Steady-State Levels of Mitochondrial tRNAs in the Heart of Tissue-Specific Knockout Mice

(A) Map indicating analyzed mitochondrial transcripts; tRNA-phe (F), tRNA-leu-UUR) (L1), tRNA-leu-CUN) (L2) and tRNA-thr (T) are transcribed by HSP, whereas tRNA-pro (P), tRNA-glu (E), tRNA-ser-UCN) (S), tRNA-tyr (Y), tRNA-cys (C), tRNA-asn (N), tRNA-ala (A) and tRNA-gln (Q) are transcribed by LSP.

(B) Northern blot analyses of mitochondrial tRNA levels in heart of control (L/L) and tissue-specific knockout (L/L, cre) mice at 16 weeks of age. (Pairs of animals analyzed, n = 6). 18S ribosomal RNA (18S) was used for loading control.

(C) Quantification of mitochondrial tRNA levels of control (white bars) and tissue-specific knockout (black bars) mice at 16 weeks of age. *$p < 0.05$; **$p < 0.01$; ***$p < 0.001$; Student's t test. All error bars indicate SEM.

gene had a promoter-distal location (Figure 5C). The levels of two tRNAs were particularly low ($tRNA^C$, ~35%, and $tRNA^Q$, ~45% of levels in controls) and can be predicted to be insufficient to sustain normal mitochondrial protein synthesis (Hayashi et al., 1991).

We studied the assembly of respiratory chain complexes by performing blue native polyacrylamide gel electrophoresis (BN-PAGE) of mitochondria from control and *Mterf3* knockout hearts at the ages of 4 and 16 weeks (Figure 6A). There was a marked reduction in levels of assembled Complex I, III, IV, and V, all of which contain mtDNA-encoded subunits, whereas Complex II, which is exclusively nucleus-encoded, was unaffected (Figure 6A). The BN-PAGE analysis also revealed a partially assembled ATP synthase subcomplex containing the α subunit. Western blot analyses showed a progressive deterioration in steady-state levels of both mtDNA- and nucleus-encoded respiratory chain subunits (Figure 6B), consistent with defective assembly of respiratory chain complexes. Measurements of respiratory chain enzyme activities in *Mterf3* knockout hearts confirmed the results from BN-PAGE analyses and showed a progressive deterioration of Complex I, Complex I–III, and Complex IV enzyme activities, whereas the Complex II enzyme activity was only slightly affected (Figure 6C). The mitochondrial ATP production rate (MAPR) in isolated mitochondria showed the same pattern of progressive impairment of respiratory chain function with time (Figure S3). There was an increase of citrate synthase activity (Figure 6C), a marker of mitochondrial mass, consistent with the increased mitochondrial mass observed by quantifying electron micrographs of *Mterf3* knockout hearts (Figure 3C).

MTERF3 Binds the mtDNA Promoter Regions and Represses Transcription Initiation

The transcriptional responses caused by lack of MTERF3 prompted us to investigate whether the protein interacts with regulatory regions of mtDNA. We established stable HeLa cell lines expressing FLAG-tagged human MTERF3 and purified this protein to homogeneity. Edman degradation sequencing showed that the mitochondrial form of MTERF3 lacked amino acids 1–68 (Figure S4A), consistent with the observed cleavage of the leader peptide after mitochondrial import (Figure 1C). Next, we expressed and purified the mitochondrial form of MTERF3 in bacteria (Figure S4B) and analyzed its DNA binding activity. Similar to MTERF1, MTERF3 displayed a strong non-sequence-specific DNA binding activity with an apparent K_d of about 16 nM (Figures S4C and S4D). However, using the electrophoresis mobility shift assay (EMSA), we detected no sequence-specific binding of MTERF3 to a set of 32 DNA fragments covering the entire human mtDNA genome in the presence of competitor DNA (poly-dI-dC) (data not shown). MTERF1 displayed sequence-specific binding to its recognition site using the same conditions (data not shown).

To further characterize MTERF3 interactions with mtDNA, we used a chromatin immunoprecipitation protocol (ChIP) in combination with 29 primer pairs to screen the entire human mtDNA genome for MTERF3 interactions (Figure 7A). The protocol was validated by using a polyclonal antiserum against human MTERF1, and as expected, we detected the previously known binding site in the $tRNA^{L1}$ gene (Figure 7B). A second MTERF1 binding site in the HSP promoter region has recently been identified (Martin et al., 2005). However, our screening did not obtain any MTERF1 signal in this area under various ChIP assay conditions (data not shown). Using a polyclonal antiserum against human MTERF3, we found a distinct and

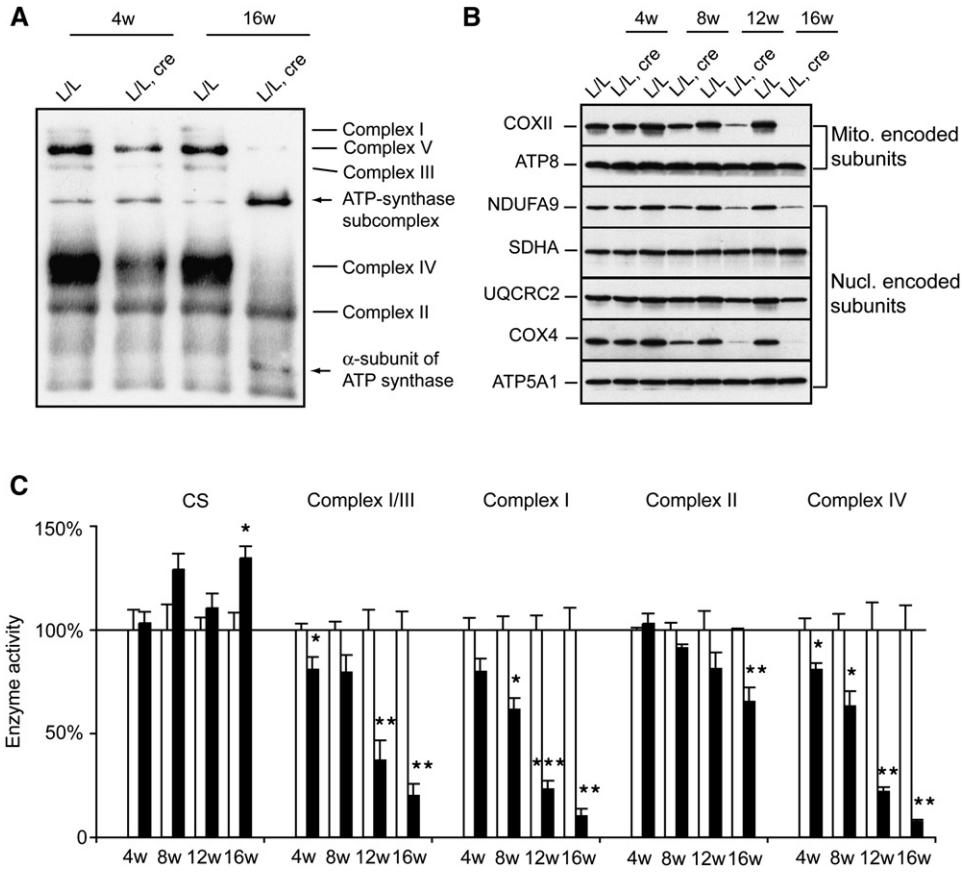

Figure 6. Defects in Respiratory Chain Function of Tissue-Specific Knockout Mice

(A) Respiratory chain enzyme complexes were analyzed by BN-PAGE in the heart of control (L/L) and tissue-specific knockout (L/L, cre) mice at 4 and 16 weeks (w) of age.

(B) Western blot analyses of subunits of respiratory chain complexes at 4, 8, 12, and 16 weeks of age. mtDNA-encoded subunits of Complex IV (COXII) and Complex V (ATP8) and nucleus-encoded subunits of Complex I (NDUFA9), Complex II (SDHA), Complex III (UQCRC2), Complex IV (COX4), and Complex V (ATP5A1) were analyzed.

(C) Relative enzyme activities of respiratory chain enzymes in the heart of tissue-specific knockout mice (black bars) and controls (white bars) at 4, 8, 12, and 16 weeks (w) of age. The enzymes are as follows: CS, citrate synthase; Complex I/III, NADH cytochrome c reductase; Complex I, NADH coenzyme Q reductase; Complex II, succinate dehydrogenase; Complex IV, cytochrome c oxidase. *$p < 0.05$; **$p < 0.01$; ***$p < 0.001$; Student's t test. All error bars indicate SEM.

reproducible increase in signal in a region containing LSP and HSP (Figure 7C). The baseline for binding of MTERF3 to all other mtDNA regions was flat and showed no additional peaks (Figure 7C). The increase in MTERF3 signal is observed over a relatively broad area and may be explained by the existence of more than one interaction site in this region. The increased levels of mtDNA transcripts in *Mterf3* knockouts and the binding of MTERF3 to the mtDNA promoters suggested that MTERF3 might affect transcription initiation. We confirmed this prediction by assessing de novo transcription of mtDNA by adding radiolabeled UTP (Figure 7D) or biotinylated UTP (Figure 7E) to isolated mitochondria from control and *Mterf3* knockout hearts. The transcription initiation was increased from both LSP and HSP in mitochondria lacking MTERF3 (Figure 7E).

The data presented above are consistent with a transcription repression role of MTERF3, and to biochemically validate this function, we monitored in vitro transcription in MTERF3-depleted human mitochondrial extracts (Figures 7F and 7G). Anti-MTERF3 antibodies depleted >90% of the MTERF3 protein, but did not affect the levels of another mitochondrial transcription factor, TFAM (Figure 7F). Depletion of MTERF3 increased transcription by ~50% in comparison with undepleted extracts (Figure 7G). Addition of recombinant MTERF3 did not restore transcription to wild-type levels, indicating that depletion of MTERF3 also leads to loss of additional factors required for MTERF3 function (data not shown).

The presented data are formally consistent with a role for MTERF3 as a promoter-proximal transcription termination factor. To address this possibility, we employed

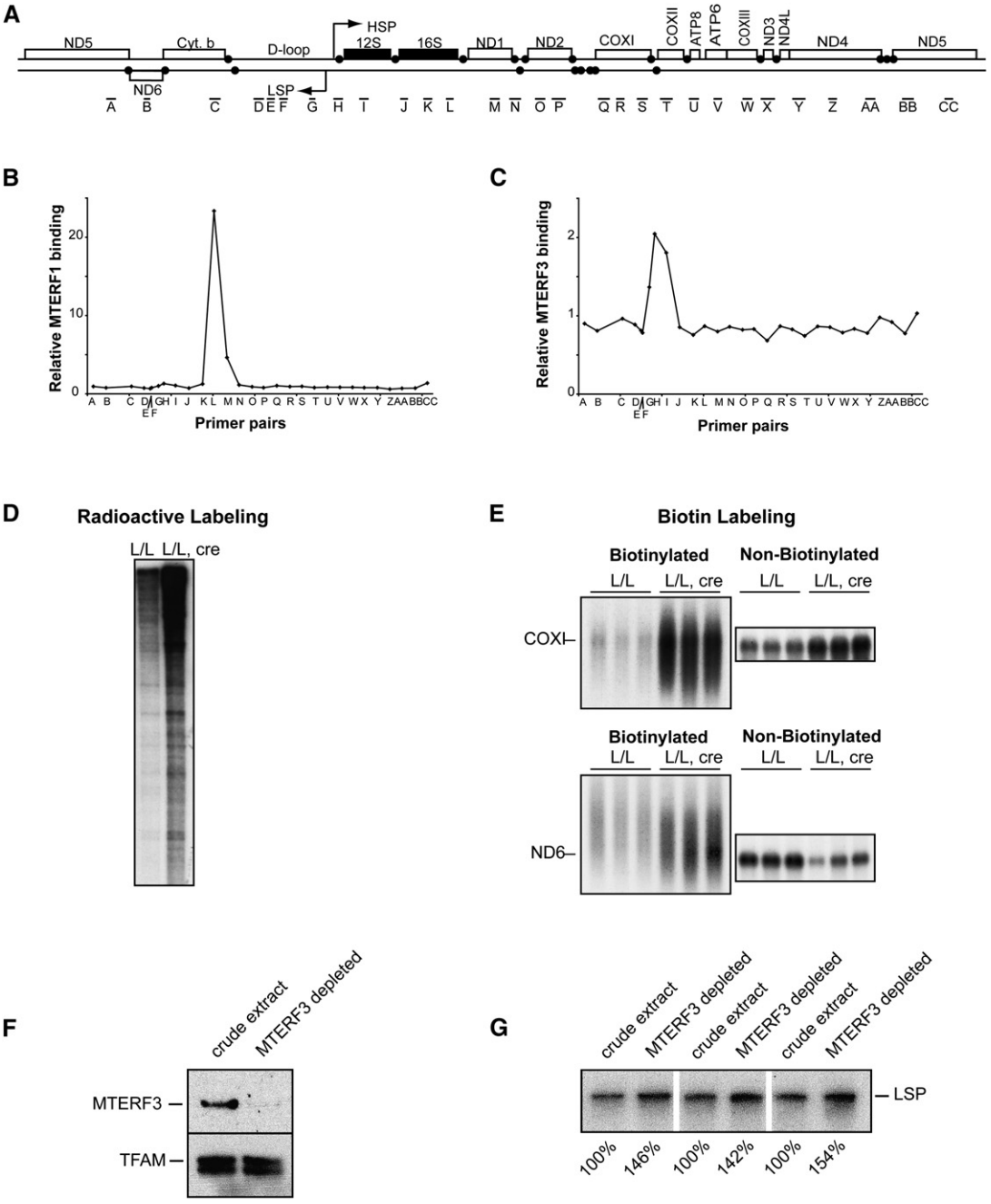

Figure 7. Interaction of MTERF3 with mtDNA

(A) Primer pairs used for chromatin immunoprecipitation (ChIP) analysis in HeLa cells.

(B) ChIP analysis with a polyclonal antibody against MTERF1.

(C) ChIP analysis with a polyclonal antibody against MTERF3.

(D) Measurement of de novo transcription of mtDNA by using radioactive UTP. Isolated mitochondria were incubated with α^{32}P-UTP and labeled transcripts were separated on polyacrylamide gels.

(E) Measurement of de novo transcription of mtDNA by using biotinylated UTP. Isolated mitochondria were incubated with biotinylated UTP and labeled transcripts were isolated by streptavidin purification and separated in denaturing agarose gels. Transcripts were detected by probing blots with radiolabeled mtDNA fragments.

(F) Immunoblot analysis of mitochondrial extracts before and after immunodepletion of MTERF3.

(G) Mitochondrial transcription is stimulated by depletion of MTERF3. Reactions carried out by S-100 mitochondrial lysate produce a specific LSP transcript. The reactions were quantified by phosphoimaging and the relative levels of transcription are shown.

northern blotting and isotope-labeled short, strand-specific oligonucleotide probes to detect promoter-proximal transcripts from LSP, HSP1, and HSP2. The rationale for this experiment is that transcription termination close to the promoters should generate short transcripts detectable by northern blot analyses. As expected, we observed increased levels of promoter-proximal transcripts in the knockout mice, but there were no additional transcript isoforms in wild-type mice (Figures S5A, S5C, and S5D). We also used S1 mapping to screen for the occurrence of promoter-proximal transcription termination events that would produce transcripts too short to be detected by northern blot analyses. This analysis was only performed on LSP transcripts. We detected higher levels of LSP promoter-proximal transcripts, but the size distribution of transcription products remained unchanged (Figure S5B). These findings argue against a role for MTERF3 in promoter-proximal transcription termination and support the interpretation that MTERF3 acts as a negative regulator of transcription initiation.

DISCUSSION

We show here that MTERF3 is a mitochondrial protein that interacts with the mtDNA promoter region and decreases transcription initiation in mammalian mitochondria. This negative regulation is likely important for fine-tuning mitochondrial transcription in response to physiological demands. Previous studies have identified ways of activating mtDNA expression, and this work shows a mechanism that is used for repression of mtDNA expression. Besides a possible regulatory physiological role, such repression could also be important in ensuring that transcription from the opposing promoters, LSP and HSP, on the small mammalian mtDNA molecule does not result in interference by collision of transcription complexes. Recent studies of nuclear transcription in yeast have demonstrated that closely spaced promoters opposing each other have normal levels of transcription initiation, but the steady-state levels of promoter-distal transcripts decrease because of transcription collision (Prescott and Proudfoot, 2002). The yeast studies have also established that decreased transcription initiation at the forward promoter will increase the steady-state levels of promoter-distal transcripts transcribed from the reverse promoter and vice versa (Prescott and Proudfoot, 2002). We found increased transcription initiation at both LSP and HSP, but decreased levels of promoter-distal LSP transcripts in MTERF3-deficient mouse hearts. The mtDNA transcription pattern in MTERF3-deficient mitochondria is thus very similar to the nuclear transcription pattern generated from opposing promoters in yeast (Prescott and Proudfoot, 2002), and it is thus possible that transcription collision is occurring in *Mterf3* knockout mice. Alternatively, the increased number of transcription initiation events may lead to a reduced availability of transcription factors, which, in turn, could affect the possibility of restarting stalled transcription and thereby reduce the levels of promoter-distal RNA molecules. Our data thus suggest that aberrant transcription causes the decrease in oxidative phosphorylation capacity in *Mterf3* knockouts and do not support the suggestion by others that MTERF3 is directly involved in regulating translation (Roberti et al., 2006).

We produced recombinant MTERF3 protein from different sources and added it to the mtDNA in vitro transcription system. However, we observed no effects after MTERF3 addition when studying in vitro transcription initiation and transcription patterns by using a variety of templates (data not shown). It is therefore likely that the action of MTERF3 is dependent on additional mitochondrial proteins besides the ones constituting the basal mitochondrial transcription machinery.

The mitochondrial transcription termination factor 1 (MTERF1, previously MTERF or MTERM) affects transcription elongation by blocking transcription downstream of the mitochondrial rRNA genes (Fernandez-Silva et al., 1997; Kruse et al., 1989; Shang and Clayton, 1994). This transcription termination action of MTERF1 has been reconstituted in a pure in vitro transcription system (Asin-Cayuela et al., 2005) and is predicted to increase the ratio of rRNAs to the downstream mRNAs. In addition, MTERF1 has been proposed to bind the HSP promoter (Martin et al., 2005). We could verify the MTERF1 binding site in the $tRNA^{L1}$ gene, but we observed no binding to the promoter region. This discrepancy from previously published results (Martin et al., 2005) could perhaps be explained by differences in protocols and sources of mitochondria for the ChIP analyses. Further understanding of MTERF1 function necessitates additional in vitro experiments as well as genetic manipulation of the MTERF1 gene in vivo.

In MTERF3-deficient hearts, we found increased levels of an unprocessed transcript containing 16S rRNA/ND1 (RNA19) and another transcript containing ND5/Cyt b sequences. Increased levels of RNA19 have been reported in patients harboring different pathogenic mutations in $tRNA^{L1}$, $tRNA^{K}$, and mtDNA deletions (Bindoff et al., 1993; Heddi et al., 1993; Koga et al., 2003). The finding of unprocessed precursor mtRNAs in MTERF3-deficient mitochondria may therefore be secondary to the respiratory-chain-deficient state or, alternatively, it may suggest an additional function for MTERF3 in RNA processing.

In conclusion, we report here that MTERF3 is an essential protein whose in vivo function is to repress transcription initiation in mammalian mitochondria. Repression of mtDNA transcription may be important in regulating oxidative phosphorylation in response to different physiological demands, and it may also provide a mechanism to avoid collision between transcription complexes generated by the opposing promoters. The discovery of the transcription inhibition role of MTERF3 will open new possibilities in studying regulation of mtDNA transcription in physiological adaptation, disease, and aging.

EXPERIMENTAL PROCEDURES

Bioinformatics Prediction of Subcellular Protein Localization, Confocal Microscopy, and Mitochondrial Protein Import Assays

See supplementary data.

Creation of *Mterf3* Knockout Mice

A targeting vector was engineered so that the exon 2 of *Mterf3*, which contains the translation start codon, was flanked by two loxP sites (Figure 2A). A loxP site was introduced in the intron 5′ to exon 2, whereas a *Frt-PGK-neo-Frt* cassette (*Frt*-site-flanked neomycin gene expressed from the phosphoglycerate kinase promoter) with an adjacent loxP site was introduced in the intron 3′ to exon 2. The targeting vector was constructed as follows: genomic clones containing the mouse *Mterf3* were isolated from a 129/SvJI FixII phage library (Stratagene). A SphI fragment of 9.8 kb containing the *Mterf3* was cloned into pBluescript II SK+ (pBS, Stratagene) to generate the plasmid pBST3. The pST7 plasmid contains an *Frt-PGK-neo-Frt* cassette and a single adjacent loxP site (Trifunovic et al., 2004). An additional BamHI site was introduced into this plasmid by ligating an oligonucleotide with a BamHI site into an XhoI site. This alteration makes it possible to excise the *Frt-PGK-neo-Frt* cassette and loxP site by BamHI digestion. This modified pST7 plasmid was digested with BamHI to excise a fragment containing the *Frt-PGK-neo-Frt* cassette and the flanking loxP site, which, in turn, was ligated into BamHI-digested pBST3 to generate pBST3neo. Next, an oligonucleotide with a PacI site was inserted into the SacI site of pST7 to allow excision of the loxP site by PacI digestion. The excised PacI fragment containing the loxP site was ligated to PacI-digested pBST3neo vector, thus creating the final knockout vector pBST3KO. The pBST3KO vector was analyzed by restriction-enzyme mapping and partial DNA sequencing for verification. The targeting vector was linearized with NotI and electroporated into 129R1 ES cells. A total of 156 ES cell clones were analyzed by Southern hybridization, and three specifically targeted clones were found. Chimeras were generated by blastocyst injection of ES cells and germline transmission was obtained from two different clones. The *Frt*-flanked *PGK-neo* gene was excised by mating *Mterf3*$^{+/neo\text{-}loxP}$ mice (Figure 2A) to transgenic mice ubiquitously expressing *Flp*-recombinase, thus generating *Mterf3*$^{+/loxP}$ mice (Figure 2A). The *Mterf3*$^{+/-}$ mice were generated by crossing *Mterf3*$^{+/loxP}$ mice to β-*actin-cre* mice ubiquitously expressing *cre*-recombinase.

Tissue-Specific Disruption of *Mterf3*

Generation of heart- and skeletal-muscle-specific *Mterf3* knockout mice was carried out as previously described (Hansson et al., 2004). *Mterf3*$^{loxP/loxP}$ mice were mated to heterozygous transgenic mice expressing *cre*-recombinase in heart and skeletal muscle (+/*Ckmm-cre*). Double heterozygous mice (*Mterf3*$^{+/loxP}$, +/*Ckmm-cre*) were obtained and crossed to *Mterf3*$^{loxP/loxP}$ mice to generate tissue-specific knockouts (*Mterf3*$^{loxP/loxP}$, +/*Ckmm-cre*). All crosses yielded offspring at the expected Mendelian proportions.

Creation of *Mterf3* BAC Transgenic Mice

A BAC clone containing *Mterf3* was identified by Clone Finder in National Center for Biotechnology Information database. A 206 kb clone (RP23-63P12) with 95 kb and 67 kb flanking sequences upstream and downstream of *Mterf3* was obtained from Children's Hospital Oakland-BAC-PAC Resources. We used BAC recombination technology (Lee et al., 2001) to alter the coding sequence of *Mterf3* so that a synonymous change was created to remove a PstI restriction enzyme site in exon 3 (Figure S1). Transgenic lines were generated from the modified BAC clone by injection of cesium chloride-purified BAC DNA into pronuclear-stage embryos of the FVB/N strain. Founders were identified by PstI-restriction enzyme analysis of a PCR product containing exon 3 of *Mterf3*. Positive transgenic lines were confirmed by Southern blot analysis of PstI-digested tail DNA by using exon 3 of *Mterf3* as probe.

Southern, Northern, and Western Blot Analyses and Antisera

Isolation of DNA, RNA, and proteins, and Southern blot, northern blot, western blot, and phosphoimager analyses were carried out as previously described (Ekstrand et al., 2004). Polyclonal rabbit antisera to mouse COXII, ATP8 were used to detect mitochondria-encoded respiratory chain subunits (Larsson et al., 1998). Monoclonal mouse antibodies detecting nucleus-encoded subunits of mouse Complex I (NDUFA9 subunit), Complex II (SDHA subunit), Complex III (UQCRC2 subunit), Complex IV (COX4 subunit), and Complex V (ATP5A1 subunit) were obtained from Molecular Probes. Pure human recombinant MTERF3 protein and two synthetic peptides of mouse MTERF3 DLSKIEKHPDAANC (amino acids 160–172) and CGRAQYDPAKPN (amino acids 368–378) were used as antigens to immunize rabbits to obtain polyclonal antisera (Agrisera AB).

Isotope-labeled oligonulceotides were used to detect promoter-proximal transcripts from LSP (5′-TCAAACCCTATGTCCTGATC-3′), HSP1 (5′-CATTTTCAGTGCTTTGCTTTGTTATTA-3′), and HSP2 (5′-TAATTATAAGGCCAGGACCAAA-3′). The nuclease S1 protection assay was performed as previously described (Martin et al., 2005) using RNA isolated from purified mitochondria and an isotope-labeled oligonucleotide probe (5′-GACATATAATATTAACTATCAAACCCTATGTCCTGATCAATTCTAGTAGT-3′).

In Vitro Transcription

Transcription competent S-100 mitochondrial lysate was prepared from a 3 liter culture of S3 HeLa cells grown to a density of 1.5 × 10^6 cells/ml in D-MEM medium (DMEM+Glutamax, Gibco, supplemented with 20 mM HEPES, 10% fetal bovine serum, 1% penicillin, and 1% streptomycin) following a previously described procedure (Micol et al., 1996). For immunodepletion, 20 μl of anti-MTERF3 in PBS was incubated together with 100 μl lysate and protein A-agarose overnight at 4°C. The mixture was passed over a Poly-Prep chromatography column (Bio-Rad, CA) and the cleared flow-through was used for immunoblot analysis and in vitro transcription. Control lysate was treated the same way, but anti-MTERF3 was replaced by PBS. In vitro transcription was performed as described in supplementary material.

Biochemistry and BN-PAGE

Mitochondria were isolated from left ventricle heart tissue of control (*Mterf3*$^{loxP/loxP}$, n = 3–5) and knockout (*Mterf3*$^{loxP/loxP}$; +/*Ckmm-cre*, n = 3–5) mice at 4, 8, 12, and 16 weeks of age, and the respiratory chain enzyme activities and the MAPR were measured blindly as described (Wibom et al., 2002).

BN-PAGE was performed on heart mitochondria from control (*Mterf3*$^{loxP/loxP}$) and tissue-specific knockout (*Mterf3*$^{loxP/loxP}$; +/*Ckmm-cre*) mice at 4 and 16 weeks of age. Heart homogenates were prepared in 150 mM KCl, 20 mM Tris-HCl, and 2 mM EDTA (pH 7.5), and centrifuged twice for 10 min at 600 × g to obtain a postnuclear supernatant. Mitochondria were pelleted by centrifugation for 20 min at 10,000 × g and resuspended in homogenization buffer supplemented with the Mini-protean protease inhibitor cocktail (Roche). Protein concentration was measured by the Bradford method. Mitochondria were resuspended in 1.75 M aminocaproic acid, 75 mM BisTris (pH 7.0), and 2 mM EDTA to a final protein concentration of 1–3 mg/ml. Resuspended mitochondria were solubilized with 1% lauryl maltoside for 15 min on ice and then centrifugued at 20,000 × g for 20 min. Supernatants consisting of 30 μg of solubilized protein were loaded in 5%–15% polyacrylamide gradient gels for BN-PAGE (Schagger and von Jagow, 1991). Proteins were transferred to a Hybond-C Extra nitrocellulose membrane (Amersham Biosciences). Western blotting was performed using antibodies (Molecular Probes) against Complex I (NDUFA9 subunit), Complex II (SDHA subunit), Complex III (UQCRC2 subunit), Complex IV (COX4 subunit), and Complex V (ATP5A1 subunit). Peroxidase-conjugated anti-mouse immunoglobulins (Amersham Biosciences) were used as secondary antibodies. The signal was detected by using ECL plus reagents (Amersham Biosciences).

MTERF3 Protein Purification and Electrophoresis Mobility Shift Assays

The cDNA encoding full-length human MTERF3 with a FLAG-tag at its carboxy terminus was cloned into pTRE-Tight (Clontech) to obtain the pTRE-FLAGT3 vector. HeLa TetOn cells (Clontech) were stably co-transfected with pTRE-FLAGT3 and a linear hygromycin resistance marker following the manufacturer's instructions. Cells were grown in monolayer in D-MEM medium supplemented with 10% fetal calf serum, 1% streptomycin, 1% penicillin, and 200 ug/ml hygromycin. Expression of hMTERF3-FLAG was induced by addition of 1 ug/ml doxycycline to the incubation medium, and cells were harvested after 48 hr of induction. Approximately 4×10^8 HeLa cells were harvested and homogenized using a Dounce Homogenizer. hMTERF3-FLAG protein was purified from mitochondria isolated by differential centrifugation using ANTI-FLAG M2 affinity gel (Sigma) according to the manufacturer's manual. Automated chemical ("Edman") protein sequencing was done using a Procise 494 instrument from Applied Biosystems (AB) as described (Tempst et al., 1994). Stepwise liberated PTH-amino acids were identified using an "on-line" HPLC system (AB) equipped with a PTH C18 (2.1 × 220 mm; 5 μm particle size) column (AB).

The mature form of MTERF3 lacking amino acids 1–68 was expressed in bacteria with a C-terminal 6×His-tag. The protein was purified to near homogeneity over Ni^{2+}-Agarose, Hi-Trap Heparin, and Mono Q (GE Healthcare). The dsDNA binding capacity of mature MTERF3 was first assayed by an EMSA using 32 different double-stranded probes of about 550 bp each covering the entire mtDNA sequence. A short 20 bp DNA fragment from the D-loop region (5′-CCACCATCCTCCGTGAAATC-3′) was chosen to analyze the nonspecific DNA interaction further. We labeled the DNA fragment in the 5′ end by using [γ-32P] ATP. Reactions were carried out in 20 μl volumes containing 10 fmol DNA template, 20 mM Tris-HCl [pH 8.0], 0.1 mM DTT, 0.1 mg/ml bovine serum albumin, 10 mM MgCl2, 10% glycerol, and the protein concentrations indicated in the figure legend. Reactions were incubated at room temperature for 15 min before separation on a 6% polyacrylamide gel in 0.5 X TBE buffer for 65 min at 150V. The gels were exposed fresh to a Phosphorimager screen and scanned with a Personal Molecular Imager FX (Bio-Rad). Quantification was carried out with Quantity One 4.6 software (Bio-Rad). The apparent K_d was calculated as described elsewhere (Carey, 1991). Identical data was obtained with recombinant MTERF3 carrying an N-terminal 6×His-tag (data not shown).

ChIP Analysis

HeLa cells grown in 15 × 175 cm tissue culture flasks to 80% confluence were harvested, washed twice in ice-cold phosphate buffered saline (PBS), and incubated in 1% formaldehyde in PBS for 10 min at room temperature. The crosslinking reaction was quenched by adding 125 mM glycine and then incubated for 5 additional minutes. After washing the cells twice in ice-cold PBS, cells were lysed and mitochondria were purified by differential centrifugation. Mitochondria were lysed as described (Micol et al., 1996) in 25 mM HEPES-KOH (pH 7.6), 10% glycerol, 5 mM $MgCl_2$, 0.5 mM EDTA, 0.5% tween-20, 0.15 M KCl, 1 mM phenylmethlsulfonylfluoride, 2 mM pepstatin A, 0.6 mM leupeptin, and 2 mM benzamidine. The mitochondrial lysate was sonicated on ice in a Bioruptor UCD 200TM (Diagenode) for 10 min at high output, with intervals of 30 s on and 30 s off, and centrifuged for 10 min at 16,000 × g. Three 100 μl aliquots of supernatant were used for each immunoprecipitation experiment. The first sample (antibody sample) was incubated with 10 μl of human MTERF3 polyclonal antibody for 2 hr in a rotary shaker at 4°C. The second sample (bead sample) was incubated in the same way with 10 μl antiserum solvent (50% glycerol, 0.02% NaN_3) without antibody, while the third sample (input sample) was not subjected to immunoprecipitation and kept on ice until the crosslinking reversal step. We added 100 μl of 50% protein A beads (Sigma) to the lysis buffer of the antibody sample and the bead sample and incubated both in a rotary shaker for 1 hr at 4°C. Next, the antibody sample and the bead sample were transferred to Ultrafree-MC filters (Millipore) and washed twice in wash buffer (50 mM HEPES-KOH [pH 7.5], 1% Triton X-100, 0.1% sodium deoxycholate, 1 mM EDTA, and 0.5 M NaCl) and twice in deoxycholate buffer (100 mM Tris-HCl [pH 8.0], 1 mM EDTA, 0.5% Na-deoxycholate, 0.5% NP-40, and 0.25 M LiCl). The antibody sample and the bead sample were rinsed in 10 mM Tris and 1 mM EDTA (pH 8.0), and the crosslinked DNA-protein complexes were eluted by incubation at 65°C for 15 min with 100 μl elution buffer (10 mM Tris, 1 mM EDTA, and 1% sodium dodecyl sulfate [pH 8.0]). At this stage, we added 200 μl elution buffer to the input sample and the protein/DNA crosslink was reverted by incubating all three samples overnight at 65°C. Proteins were removed by incubating with 20 μg proteinase K for 2 hr at 56°C. DNA was extracted once with phenol/chloroform/isoamylalcohol (25:24:1) and once with chloroform and precipitated overnight at −20°C with 2.5 volumes of ethanol in the presence of 0.2 M NaCl and 20 μg glycogen. Quantitative PCR was carried out on a LightCycler 2.0 Instrument (Roche) using the LightCycler FastStart DNA Master SYBR Green I kit. The PCR reactions were carried out according to the manufacturer's instructions. The primer pairs used for ChIP are listed in Table S1 in the Supplemental Data (available with this article online). For each pair of primers, a calibration curve was calculated with five standards of known concentrations of human mtDNA (1.4 nM, 0.14 nM, 14 fM, 1.4 fM, and 0.14 fM). The crossing point was calculated for each sample and interpolated with the calibration curve to obtain the DNA concentration. Results were expressed as the ratio between the concentration of DNA calculated for the antibody sample and that calculated for the bead sample (signal/noise ratio).

In Organello Transcription Assay

De novo transcription was measured in isolated mitochondria as described previously (Enriquez et al., 1996). The mitochondrial fraction was suspended in transcription buffer containing 25 mM sucrose, 75 mM sorbitol, 100 mM KCl, 10 mM K_2HPO_4, 50 mM EDTA, 5 mM $MgCl_2$, 1 mM ADP, 10 mM glutamate, 2.5 mM malate, and 10 mM Tris-HCl (pH7.4), with 1 mg of BSA per ml. Mitochondria containing a total of 200 μg protein were incubated in 300 μl of the transcription buffer containing 10 mCi of α^{32}P-UTP (Amersham Biosciences) at 37°C for 30 min. After the incubation, the mitochondria were pelleted and washed with PBS. The mitochondria were then solubilized in 100 ml of lysis buffer containing 50 mM Tris-HCl (pH 8.0), 20 mM NaCl, 1 mM EDTA, 1% SDS, and 20 mg of protease K (Gibco), and then incubated at room temperature for 15 min. The mitochondrial RNA was isolated by phenol extraction. Mitochondrial RNA was labeled with biotin by using 2 μl of 10 mM Bio-11-UTP (Ambion) and using the same procedure.

Supplemental Data

The Supplemental Data for this article can be found online at http://www.cell.com/cgi/content/full/130/2/273/DC1/.

ACKNOWLEDGMENTS

This study was supported by the Swedish Research Council, the Swedish Heart and Lung Foundation, the Torsten and Ragnar Söderbergs Foundation, The LeDucq Foundation, The Swedish Cancer Society, European Commission (fp6 EUMITOCOMBAT), The Swedish Strategic Foundation (INGVAR), and Knut and Alice Wallenbergs Stiftelse. We thank Neal G. Copeland for the kind gift of plasmids for the engineering of BAC clones.

We dedicate this paper to the memory of Rolf Luft (1914–2007), who founded the field of mitochondrial medicine.

Received: December 13, 2006
Revised: April 11, 2007
Accepted: May 18, 2007
Published: July 26, 2007

REFERENCES

Asin-Cayuela, J., Schwend, T., Farge, G., and Gustafsson, C.M. (2005). The human mitochondrial transcription termination factor (mTERF) is fully active in vitro in the non-phosphorylated form. J. Biol. Chem. *280*, 25499–25505.

Bindoff, L.A., Howell, N., Poulton, J., McCullough, D.A., Morten, K.J., Lightowlers, R.N., Turnbull, D.M., and Weber, K. (1993). Abnormal RNA processing associated with a novel tRNA mutation in mitochondrial DNA. J. Biol. Chem. *268*, 19559–19564.

Carey, J. (1991). Gel retardation. Methods Enzymol. *208*, 103–117.

Dairaghi, D.J., Shadel, G.S., and Clayton, D.A. (1995). Addition of a 29 residue carboxyl-terminal tail converts a simple HMG box-containing protein into a transcriptional activator. J. Mol. Biol. *249*, 11–28.

Ekstrand, M.I., Falkenberg, M., Rantanen, A., Park, C.B., Gaspari, M., Hultenby, K., Rustin, P., Gustafsson, C.M., and Larsson, N.G. (2004). Mitochondrial transcription factor A regulates mtDNA copy number in mammals. Hum. Mol. Genet. *13*, 935–944.

Enriquez, J.A., Perez-Martos, A., Lopez-Perez, M.J., and Montoya, J. (1996). In organello RNA synthesis system from mammalian liver and brain. Methods Enzymol. *264*, 50–57.

Falkenberg, M., Gaspari, M., Rantanen, A., Trifunovic, A., Larsson, N.G., and Gustafsson, C.M. (2002). Mitochondrial transcription factors B1 and B2 activate transcription of human mtDNA. Nat. Genet. *31*, 289–294.

Fernandez-Silva, P., Martinez-Azorin, F., Micol, V., and Attardi, G. (1997). The human mitochondrial transcription termination factor (mTERF) is a multizipper protein but binds to DNA as a monomer, with evidence pointing to intramolecular leucine zipper interactions. EMBO J. *16*, 1066–1079.

Gaspari, M., Falkenberg, M., Larsson, N.G., and Gustafsson, C.M. (2004). The mitochondrial RNA polymerase contributes critically to promoter specificity in mammalian cells. EMBO J. *23*, 4606–4614.

Hance, N., Ekstrand, M.I., and Trifunovic, A. (2005). Mitochondrial DNA polymerase gamma is essential for mammalian embryogenesis. Hum. Mol. Genet. *14*, 1775–1783.

Hansson, A., Hance, N., Dufour, E., Rantanen, A., Hultenby, K., Clayton, D.A., Wibom, R., and Larsson, N.G. (2004). A switch in metabolism precedes increased mitochondrial biogenesis in respiratory chain-deficient mouse hearts. Proc. Natl. Acad. Sci. USA *101*, 3136–3141.

Hayashi, J.-I., Ohta, S., Kikuchi, A., Takemitsu, M., Goto, Y.-I., and Nonaka, I. (1991). Introduction of disease-related mitochondrial DNA deletions into HeLa cells lacking mitochondrial DNA results in mitochondrial dysfunction. Proc. Natl. Acad. Sci. USA *88*, 10614–10618.

Heddi, A., Lestienne, P., Wallace, D.C., and Stephien, G. (1993). Mitochondrial DNA expression in mitochondrial myopathies and coordinated expression of nuclear genes involved in ATP production. J. Biol. Chem. *268*, 12156–12163.

Koga, A., Koga, Y., Akita, Y., Fukiyama, R., Ueki, I., Yatsuga, S., and Matsuishi, T. (2003). Increased mitochondrial processing intermediates associated with three tRNA(Leu(UUR)) gene mutations. Neuromuscul. Disord. *13*, 259–262.

Kruse, B., Narasimhan, N., and Attardi, G. (1989). Termination of transcription in human mitochondria: identification and purification of a DNA binding protein factor that promotes termination. Cell *58*, 391–397.

Larsson, N.G., Wang, J., Wilhelmsson, H., Oldfors, A., Rustin, P., Lewandoski, M., Barsh, G.S., and Clayton, D.A. (1998). Mitochondrial transcription factor A is necessary for mtDNA maintenance and embryogenesis in mice. Nat. Genet. *18*, 231–236.

Lee, E.C., Yu, D., Martinez de Velasco, J., Tessarollo, L., Swing, D.A., Court, D.L., Jenkins, N.A., and Copeland, N.G. (2001). A highly efficient Escherichia coli-based chromosome engineering system adapted for recombinogenic targeting and subcloning of BAC DNA. Genomics *73*, 56–65.

Li, H., Wang, J., Wilhelmsson, H., Hansson, A., Thorén, P., Duffy, J., Rustin, P., and Larsson, N.G. (2000). Genetic modification of survival in tissue-specific knockout mice with mitochondrial cardiomyopathy. Proc. Natl. Acad. Sci. USA *97*, 3467–3472.

Lin, J., Wu, P.H., Tarr, P.T., Lindenberg, K.S., St-Pierre, J., Zhang, C.Y., Mootha, V.K., Jager, S., Vianna, C.R., Reznick, R.M., et al. (2004). Defects in adaptive energy metabolism with CNS-linked hyperactivity in PGC-1alpha null mice. Cell *119*, 121–135.

Lin, J., Handschin, C., and Spiegelman, B.M. (2005). Metabolic control through the PGC-1 family of transcription coactivators. Cell Metab. *1*, 361–370.

Lin, M.T., and Beal, M.F. (2006). Mitochondrial dysfunction and oxidative stress in neurodegenerative diseases. Nature *443*, 787–795.

Linder, T., Park, C.B., Asin-Cayuela, J., Pellegrini, M., Larsson, N.G., Falkenberg, M., Samuelsson, T., and Gustafsson, C.M. (2005). A family of putative transcription termination factors shared amongst metazoans and plants. Curr. Genet. *48*, 265–269.

Martin, M., Cho, J., Cesare, A.J., Griffith, J.D., and Attardi, G. (2005). Termination factor-mediated DNA loop between termination and initiation sites drives mitochondrial rRNA synthesis. Cell *123*, 1227–1240.

Micol, V., Fernandez-Silva, P., and Attardi, G. (1996). Isolation and assay of mitochondrial transcription termination factor from human cells. Methods Enzymol. *264*, 158–173.

Parisi, M.A., and Clayton, D.A. (1991). Similarity of human mitochondrial transcription factor 1 to high mobility group proteins. Science *252*, 965–969.

Prescott, E.M., and Proudfoot, N.J. (2002). Transcriptional collision between convergent genes in budding yeast. Proc. Natl. Acad. Sci. USA *99*, 8796–8801.

Roberti, M., Bruni, F., Loguercio Polosa, P., Manzari, C., Gadaleta, M.N., and Cantatore, P. (2006). MTERF3, the most conserved member of the mTERF-family, is a modular factor involved in mitochondrial protein synthesis. Biochim. Biophys. Acta *1757*, 1199–1206.

Rodriguez, C.I., Buchholz, F., Galloway, J., Sequerra, R., Kasper, J., Ayala, R., Stewart, A.F., and Dymecki, S.M. (2000). High-efficiency deleter mice show that FLPe is an alternative to Cre- loxP. Nat. Genet. *25*, 139–140.

Scarpulla, R.C. (2006). Nuclear control of respiratory gene expression in mammalian cells. J. Cell. Biochem. *97*, 673–683.

Schagger, H., and von Jagow, G. (1991). Blue native electrophoresis for isolation of membrane protein complexes in enzymatically active form. Anal. Biochem. *199*, 223–231.

Seidel-Rogol, B.L., McCulloch, V., and Shadel, G.S. (2003). Human mitochondrial transcription factor B1 methylates ribosomal RNA at a conserved stem-loop. Nat. Genet. *33*, 23–24.

Shang, J., and Clayton, D.A. (1994). Human mitochondrial transcription termination exhibits RNA polymerase independence and biased bipolarity in vitro. J. Biol. Chem. *269*, 29112–29120.

Smeitink, J., van Den Heuvel, L., and DiMauro, S. (2001). The genetics and pathology of oxidative phosphorylation. Nat. Rev. Genet. *2*, 342–352.

Tempst, P., Geromanos, S., Elicone, C., and Erdjument-Bromage, H. (1994). Improvements in microsequencer performance for low picomole sequence analysis. METHODS Companion Meth. Enzymol. *6*, 248–261.

Trifunovic, A. (2006). Mitochondrial DNA and ageing. Biochim. Biophys. Acta *1757*, 611–617.

Trifunovic, A., Wredenberg, A., Falkenberg, M., Spelbrink, J.N., Rovio, A.T., Bruder, C.E., Bohlooly-Y, M., Gidlöf, S., Oldfors, A., Wibom, R., et al. (2004). Premature ageing in mice expressing defective mitochondrial DNA polymerase. Nature *429*, 417–423.

Wang, J., Wilhelmsson, H., Graff, C., Li, H., Oldfors, A., Rustin, P., Brüning, J.C., Kahn, C.R., Clayton, D.A., Barsh, G.S., et al. (1999). Dilated cardiomyopathy and atrioventricular conduction blocks induced by heart-specific inactivation of mitochondrial DNA gene expression. Nat. Genet. *21*, 133–137.

Wibom, R., Hagenfeldt, L., and von Döbeln, U. (2002). Measurement of ATP production and respiratory chain enzyme activities in mitochondria isolated from small muscle biopsy samples. Anal. Biochem. *311*, 139–151.

Wredenberg, A., Wibom, R., Wilhelmsson, H., Graff, C., Wiener, H.H., Burden, S.J., Oldfors, A., Westerblad, H., and Larsson, N.G. (2002). Increased mitochondrial mass in mitochondrial myopathy mice. Proc. Natl. Acad. Sci. USA *99*, 15066–15071.

Wu, Z., Puigserver, P., Andersson, U., Zhang, C., Adelmant, G., Mootha, V., Troy, A., Cinti, S., Lowell, B., Scarpulla, R.C., and Spiegelman, B.M. (1999). Mechanisms controlling mitochondrial biogenesis and respiration through the thermogenic coactivator PGC-1. Cell *98*, 115–124.